

## Original Research

# Characterization of *Demodex musculi* Infestation, Associated Comorbidities, and Topographic Distribution in a Mouse Strain with Defective Adaptive Immunity

Melissa A Nashat,<sup>1</sup> Kerith R Luchins,<sup>2</sup> Michelle L Lephert,<sup>3,†</sup> Elyn R Riedel,<sup>4</sup> Joanna N Izdebska,<sup>5</sup> and Neil S Lipman<sup>1,3,\*</sup>

A colony of B6.Cg-*Rag1*<sup>tm1Mom</sup> *Tyrrp1*<sup>B-w</sup> Tg(*Tcra*,*Tcrb*)9Rest (TRP1/TCR) mice presented with ocular lesions and ulcerative dermatitis. Histopathology, skin scrapes, and fur plucks confirmed the presence of *Demodex* spp. in all clinically affected and subclinical TRP1/TCR mice examined ( $n = 48$ ). *Pasteurella pneumotropica* and *Corynebacterium bovis*, both opportunistic pathogens, were cultured from the ocular lesions and skin, respectively, and bacteria were observed microscopically in abscesses at various anatomic locations (including retroorbital sites, tympanic bullae, lymph nodes, and reproductive organs) as well as the affected epidermis. The mites were identified as *Demodex musculi* using the skin fragment digestion technique. Topographic analysis of the skin revealed mites in almost all areas of densely haired skin, indicating a generalized demodecosis. The percentage of infested follicles in 8- to 10-wk-old mice ranged from 0% to 21%, and the number of mites per millimeter of skin ranged from 0 to 3.7. The head, interscapular region, and middorsum had the highest proportions of infested follicles, ranging from 2.3% to 21.1% (median, 4.9%), 2.0% to 16.6% (8.1%), and 0% to 17% (7.6%), respectively. The pinnae and tail skin had few or no mites, with the proportion of follicles infested ranging from 0% to 3.3% (0%) and 0% to 1.4% (0%), respectively. The number of mites per millimeter was strongly correlated with the percentage of infested follicles. After administration of amoxicillin-impregnated feed (0.12%), suppurative infections were eliminated, and the incidence of ulcerative dermatitis was dramatically reduced. We hypothesize that the *Rag1*-null component of the genotype makes TRP1/TCR mice susceptible to various opportunistic infestations and infections, including *Demodex* mites, *P. pneumotropica*, and *C. bovis*. Therefore, *Rag1*-null mice may serve as a useful model to study human and canine demodecosis. *D. musculi* should be ruled out as a contributing factor in immunocompromised mouse strains with dermatologic manifestations.

**Abbreviations:** NK, natural killer; NSG, NOD.Cg-*Prkdc*<sup>scid</sup> *Il2rg*<sup>tm1Wjl</sup>/Sz; *Rag*, recombination activating gene; TRP1/TCR, B6.Cg-*Rag1*<sup>tm1Mom</sup> *Tyrrp1*<sup>B-w</sup> Tg(*Tcra*,*Tcrb*)9Rest; UD, ulcerative dermatitis

Immunocompromised mouse models are increasingly used in a variety of scientific disciplines, most notably cancer biology, because they readily support the growth of human tumors. Unfortunately, these models pose challenges in that they are susceptible to opportunistic pathogens, including bacteria and parasites. Recently, an immunocompromised mouse strain maintained at our institution, B6.Cg-*Rag1*<sup>tm1Mom</sup> *Tyrrp1*<sup>B-w</sup> Tg(*Tcra*,*Tcrb*)9Rest/M (TRP1/TCR) mice, presented with pruritus, ulcerative dermatitis (UD), and ocular lesions, including exophthalmia, which were

attributed to opportunistic bacterial infections and infestation with *Demodex* mites.

TRP1/TCR mice are a transgenic strain expressing an MHC class II-restricted T-cell receptor that recognizes the endogenous melanocyte differentiation antigen minimal tyrosinase-related protein 1 (TRP1) epitope.<sup>62</sup> These mice serve as a source of melanocyte-reactive CD4<sup>+</sup> T lymphocytes and are useful in cancer research.<sup>53,62,69</sup> They harbor 3 genetic alterations: a Y chromosome insertion of an MHC-restricted T-cell receptor (expressed only in males); a radiation-induced mutation of TRP1 (called the white-based brown allele), resulting in a brown coat color; and a targeted deletion of recombination activating gene 1 (*Rag1*).<sup>62</sup> RAG1-deficient mice lack mature T and B lymphocytes, thus altering the adaptive immune response.<sup>57</sup>

*Demodex* mites are small, cigar-shaped ectoparasites that principally reside in hair follicles and adnexal glands of mammals, where they feed and reproduce. *Demodex* spp. are prostigmatid mites in the Demodecidae family and belong to the superfamily of Cheyletoidea; they are most closely related to mites in the

Received: 28 Dec 2016. Revision requested: 22 Jan 2017. Accepted: 06 Feb 2017.

<sup>1</sup>Tri-Institutional Training Program in Laboratory Animal Medicine and Science, Memorial Sloan Kettering Cancer Center, Weill Cornell Medicine, and The Rockefeller University, New York, New York; <sup>2</sup>Animal Resources Center, The University of Chicago, Chicago, Illinois; <sup>3</sup>Center for Comparative Medicine and Pathology, Memorial Sloan Kettering Cancer Center and Weill Cornell Medicine, New York, New York; <sup>4</sup>Epidemiology and Biostatistics Department, Memorial Sloan Kettering Cancer Center, New York, New York; and <sup>5</sup>Department of Invertebrate Zoology and Parasitology, University of Gdansk, Gdansk, Poland.

<sup>†</sup>Current affiliation: Gribbles Veterinary, Christchurch, New Zealand

\*Corresponding author. Email: lipmann@mskcc.org

families Cheyletidae and Psorergatidae, namely *Cheyletiella* spp. and *Psorergates* spp., respectively.<sup>6,28</sup> All mite stages live within the pilosebaceous unit. As is typical with acarine ontogeny, life stages for *D. musculi* include the ovum (egg), hexapod larva, hexapod nymphal stage (protonymph), octopod nymphal stage (deutonymph), and adults (males and females).<sup>28</sup> Mites use their mouth parts (chelicerae) to puncture epithelial and sebaceous cells for feeding.<sup>19</sup>

*Demodex* mites are generally host-specific and have been identified in wild and domesticated species, including laboratory animals.<sup>79</sup> Of the more than 120 species of *Demodex* that have been characterized, more than 25% have been described in wild or captive rodents, including *Mus musculus*.<sup>28,31,32,34-36,39,40,43,63,65,93</sup> In normal healthy animals, *Demodex* mites exist in low numbers and are considered commensal microfauna, but immunocompromised mammals may develop clinical disease.<sup>28</sup> In humans, 2 species of mites, *D. folliculorum* and *D. brevis*, contribute to dermatologic and ocular conditions, especially in immunocompromised patients.<sup>24,49,91,92</sup> Although clinical signs resulting from *Demodex* infestations are common in some veterinary species, such as dogs and hamsters,<sup>18,30,35,61,65</sup> *Demodex* mites are rarely reported in laboratory mice.<sup>26,27,50,85</sup> Since a 1919 characterization of various *Demodex* species, the only species identified, to date, in laboratory mice has been *D. musculi*.<sup>26-28,50,85</sup> In mice, immune deficiency has contributed to mite susceptibility, and clinical signs are sometimes apparent.<sup>27,50</sup> In addition, laboratory mice have been used as animal models to study demodocosis.<sup>13,87</sup> The most common mode of transmission of *Demodex* mites is by direct contact, typically from dam to offspring.<sup>9,27</sup> Commercially available laboratory mice, which are offspring from animals obtained by Cesarean rederivation, are presumably free of *Demodex* mites.<sup>68</sup>

Here, we describe the diagnosis, species identification, and topographic distribution of *D. musculi*, a seemingly rare ectoparasite, and associated opportunistic infections in an immunocompromised transgenic mouse strain with a deficiency in adaptive immunity. We posit that *Demodex* mites may be more common than previously recognized and that immunocompromised mice are at risk of high mite burdens and are more likely to develop clinical ramifications from infestation.

## Materials and Methods

**Animals.** The TRP1/TCR strain was generated by Nicholas Restifo and, in 2006, 2 breeding pairs were imported to our institution's quarantine facility from the National Cancer Institute.<sup>62</sup> Two of the 4 original TRP1/TCR imported mice were dead on arrival, and one died shortly after arrival. Two carcasses were not evaluated, because their tissues were extremely autolyzed; the third underwent complete necropsy. The surviving male was sent to the Memorial Sloan Kettering Cancer Center's Mouse Genetics Core for sperm harvest to rescue the line by *in vitro* fertilization. Superovulated, vendor-sourced mice were used as a source of ova for *in vitro* fertilization. At the Memorial Sloan Kettering Cancer Center, all colonies are SPF for mouse hepatitis virus, Sendai virus, mouse parvoviruses 1 and 2, minute virus of mice, pneumonia virus of mice, Theiler meningoencephalitis virus, epizootic diarrhea of infant mice (mouse rotavirus), ectromelia virus, reovirus type 3, lymphocytic choriomeningitis virus, K virus, mouse adenovirus types 1 and 2, polyoma virus, murine cytomegalovirus, mouse thymic virus, and Hantaan virus; *Mycoplasma pulmonis*, *Citrobacter rodentium*, *Salmonella* spp., ciliary-associated

respiratory bacillus, and *Clostridium piliforme*; and fur mites (*Myobia musculi*, *Myocoptes musculinus*, and *Radfordia affinis*), pinworms (*Syphacia* and *Aspicularis* spp.), and *Encephalitozoon cuniculi*.<sup>11,72</sup>

After rescue by *in vitro* fertilization, the resultant TRP1/TCR mice were crossed with 2 different lines to generate 3 additional strains: 1) green fluorescent protein fused to the regulatory T-cell transcription factor, FoxP3 (FoxP3-GFP strain); 2) SJL-luciferase (on B6.SJL background) for use in imaging studies; and 3) both reporter genes. The exact genotypes of the mice used for breeding were not available, but in light of the strain name, they are likely C57BL/6-Tg(Foxp3-GFP)90Pkraj and B6.SJL-Ptprca/BoyAi, respectively. The parental strain was maintained in the colony also. At the time of presentation, the colony consisted of approximately 80 cages of the parental TRP1/TCR strain and an additional 120 cages of the various TRP1/TCR reporter strains. Over the course of 1 y, 48 mice of the TRP1/TCR parental strain and 9 mice from the 3 reporter strains were evaluated from the breeding colony.

In addition, TRP1/TCR mice were purchased from The Jackson Laboratory (Bar Harbor, ME) to establish a second, mite-free TRP1/TCR colony. Mice of both colonies were housed in breeding pairs or trios in IVC (Thoren Caging Systems, Hazelton, PA) in separate rooms. The cages were maintained under positive pressure with regard to the holding room. Mice were fed a  $\gamma$ -irradiated diet (PicoLab Mouse Diet 5053, Purina LabDiet, St. Louis, MO) without restriction, received acidified water (pH 2.5 to 2.8) in polysulfone bottles with neoprene stoppers (Techniplast, West Chester, PA), were housed in polysulfone cages (no. 19; Thoren Caging Systems) on autoclaved aspen chip bedding (PWI Industries, Quebec, Canada), and were maintained on a 12:12-h light:dark cycle, with room humidity ranging from 30% to 70% and room temperature at  $72.0 \pm 2.0$  °F ( $22.2 \pm 1.0$  °C). Cage bottoms and bedding were changed weekly, and the remaining cage components (wire bar lid and bottle) were changed every other week. The maintenance and experimental use of mice were approved by the the Memorial Sloan Kettering Cancer Center IA-CUC. The animal care and use program is AAALAC-accredited and operates in adherence with the *Guide for the Care and Use of Laboratory Animals*, 8th edition.<sup>42</sup>

**Clinical history.** In 2013, within 3 mo of being transferred from a barrier breeding facility into an experimental facility maintained in a different barrier vivarium, numerous TRP1/TCR mice from a breeding colony presented with skin and ocular lesions. The 2 facilities were within the same institution, but were physically separated by approximately 3 miles, and they used different husbandry and veterinary technical staff. Breeding of rodents occurred at both facilities. The standard personal protective equipment used in both facilities included a disposable gown, a hair bonnet, and disposable gloves. Prior to facility entry, an automated shoe cleaner was used in both facilities. In addition, entry into the experimental facility occurred through an air shower.

After several mice were euthanized due to the severity of their lesions, a thorough clinical investigation was initiated, and a series of animals were submitted for necropsy and microbiologic assessment. Of the 48 TRP1/TCR mice evaluated from the breeding colony, 22 (46%) were male, and 26 (54%) were female. The median age at euthanasia was 104 d (range, 56 to 852 d) for cases in which the animals' ages were known ( $n = 45$ ). Male mice ranged in age from 67 to 852 d (median, 94 d), and female mice were 83 to 773 d (median, 104 d) old.

**Anatomic pathology.** Mice were euthanized by carbon dioxide asphyxiation in adherence with the recommendations in the *AVMA Guidelines on Euthanasia of Animals*, 2013 edition.<sup>5</sup> Parental TRP1/TCR mice ( $n = 48$ ) and reporter substrains ( $n = 3$ ) were submitted to the Memorial Sloan Kettering Cancer Center's Laboratory of Comparative Pathology for gross necropsy and ectoparasite examination. A subset of animals, including both the parental ( $n = 6$ ) and reporter strains ( $n = 3$ ), underwent complete necropsy. Tissues evaluated included heart, lungs, trachea, thymus, tracheal lymph nodes, spleen, mesenteric lymph nodes, bone marrow, pancreas, adrenals, thyroid, salivary glands, esophagus, stomach, intestines, liver, gall bladder, kidneys, urinary bladder, uterus, ovaries, cervix and vagina or testes, epididymides, seminal vesicles and prostate, stifle joint, sternum, femur, vertebral column, skin (head and ventrum), and spinal column. Coronal sections of the head yielded tissues of the eyes, nasal cavity, oral cavity, ear canals, and brain. Tissues were fixed in 10% neutral-buffered formalin. Bones were decalcified in a mixture of formaldehyde, formic acid, and methanol (Decalcifier I solution, Leica Biosystems, Richmond, IL) for 72 to 96 h and then were washed with copious amounts of tap water for 20 min. Tissues were processed routinely, and sections (thickness, 4  $\mu\text{m}$ ) were stained with hematoxylin and eosin. Histopathologic assessment was performed by a board-certified veterinary pathologist.

**Bacteriology.** At necropsy, sterile cotton-tip applicators (BactiSwab, Remel, Lenexa, KS) were used to collect samples from skin (with a focus on the muzzle area) and abscesses of 6 TRP1/TCR parental and 3 reporter-strain mice to identify aerobic microorganisms. Samples were plated on trypticase soy agar II with 5% sheep blood, Columbia colistin–nalidixic acid agar with 5% sheep blood, and chocolate II agar plates (BBL, BD Diagnostic Systems, Sparks, MD). Plates were incubated aerobically at 37 °C in 5% CO<sub>2</sub> for as long as 7 d. Colonies were isolated, subcultured on trypticase soy agar II plates, and incubated for 24 to 48 h. Subsequently, bacterial isolates were identified by using colorimetric biochemical tests (API Coryne and API 20 NE, bioMérieux, Marcy L'Etoile, France).

**Parasitology and *Demodex* mite identification.** Forty-six TRP1/TCR mice from the breeding colony and 9 reporter-strain mice were tested for ectoparasites by fur pluck and deep skin scrape. Most animals were tested immediately after euthanasia; one parental strain mouse and 6 reporter-strain mice were not euthanized but were maintained in the colony. Fur plucks, collected from the face, interscapular region, caudal dorsum, and ventrum, were performed by grasping a small clump of hairs in a 5-in. curved mosquito hemostat, then rapidly pulling perpendicularly to the skin's surface while the rodent was restrained manually. This process was repeated 3 or 4 times in the same region to ensure an adequate sample. Hairs from a single anatomic site were placed in a drop of mineral oil on a glass slide and cover-slipped. Hemostats were dipped in 70% ethyl alcohol or were thoroughly washed with detergent and water between mice. Deep skin scrapes were performed on the interscapular region and caudal dorsum and ventrum by first squeezing the region of skin to be sampled between the collector's thumb and index finger while the mouse was manually restrained; then, using a no. 10 or 20 sterile scalpel blade, the area was scraped opposite the direction of hair growth, with firm pressure applied to the skin. The debris collected on the blade was placed in mineral oil on a microscope slide and cover-slipped. In addition to fur plucks, deep skin scrapes were selected for ectoparasite testing because of the

mites' presence within hair follicles. On most mice, additional ectoparasite tests, including superficial skin scrapes and tape impression tests, were performed as previously described.<sup>71,84</sup> All skin samples were evaluated for parasites under 100 to 200 $\times$  magnification (Olympus CX31 binocular microscope, Waltham, MA) by a trained veterinarian. Observation of mice during and after ectoparasite testing indicated that testing caused momentary discomfort, mainly due to restraint. After testing, live mice displayed normal behaviors, with increased grooming due to residual mineral oil on the animals' fur.

To identify the mite species, additional TRP1/TCR mice ( $n = 4$ , adult, parental strain mice) were euthanized. Pelts were harvested and were processed according to the skin fragment digestion method.<sup>37</sup> The pelts were removed by incising the skin from the perineum to the ventral cervical region along the midline, with annular incisions made around the carpi and tarsi. The caudal vertebrae were sharply incised, and the skin was peeled back in a caudal to cranial direction. The palpebrae, vibrissae, and pinnae were incised to remove the skin of the head and muzzle. Each pelt was placed on a 5  $\times$  10 cm piece of cardboard and placed in 50 mL 70% ethanol at 4 °C. Fixation alcohol was replaced with fresh alcohol for storage after 48 to 72 h. Whole skin fragments (approximately 0.5 to 1 cm<sup>2</sup>) were harvested from approximately 15 anatomic locations including the head (ears, periocular region, eyes, vibrissae, nose, and muzzle), interscapular region, ventrum, dorsum, limbs, perineal region, and tail from each pelt and digested in separate conical centrifuge tubes at room temperature for a maximum of 5 d, depending on the thickness of the skin, in 10% potassium hydroxide solution. The lysate was centrifuged at 3500 rpm (1139  $\times$  g) for 10 min and decanted; 20  $\mu\text{L}$  of lysate was placed on a microscope slide and mounted in polyvinyl lactophenol solution. Parasites were examined at 1000 $\times$  magnification under phase contrast microscopy (Eclipse 50i, Nikon, Tokyo, Japan). For mite identification, 50 to 100 specimens of each life stage were identified, measured, and photographed by a trained parasitologist.

**Skin topography of *Demodex* mites.** To determine the distribution of *Demodex* mites in various anatomic regions, skin topography was performed on 8- to 10-wk-old TRP1/TCR mice ( $n = 10$ , 5 male and 5 female) from the breeding colony. After euthanasia, the pelt, including the skin of the head and tail, was removed as described earlier. The pelt was adhered to a 5  $\times$  10 cm piece of cardboard for fixation in 10% neutral-buffered formalin and sectioning. Skin specimens ( $n = 22$ ; length, 0.5 to 1 cm; width, 2 to 3 mm) were sectioned from 13 anatomic regions of each of the 10 mice. Regions of skin collected included the nose and vibrissae, interocular, pinnae, head, interscapular, cranial ventrum, mid ventrum, caudal ventrum, mid dorsum, caudal dorsum, limbs, perineum, and tail. Samples from distinct regions were identified with tissue marking dyes and placed in tissue embedding cassettes. Skin was embedded in paraffin, and tissue blocks were sectioned (thickness, 4  $\mu\text{m}$ ) by using a microtome, placed on microscope slides, and stained with hematoxylin and eosin. A subset of sections from several mice were stained with Luna stain as described to determine whether the chitinous exoskeleton of *D. musculi* would be enhanced with a histochemical stain for chitin.<sup>52</sup>

The number of mites in each stained section was counted (magnification, 200 to 400 $\times$ ). All transverse, longitudinal, and oblique sections of hair follicles visible in the dermis and epidermis were counted, and the length of the skin sections was recorded in millimeters. The percentage of infested follicles was calculated by

dividing the number of follicular sections containing mites by the total number of follicular sections observed and multiplying by 100%. The number of mites per length of skin was determined by dividing the number of mites by the length of the skin section in millimeters. Single skin sections were analyzed from selected anatomic regions (that is, head and tail), whereas other, larger anatomic regions (dorsum and ventrum) or those that were bilateral (limbs and pinnae) had multiple skin sections analyzed and the values were combined by region for analysis. The data are displayed as the median (central line), with the first and third quartiles indicated by the boxes and the upper and lower limits of the ranges bounded by the whiskers.

**Epidemiologic investigation to ascertain source of mites.** Tissues were evaluated from only 1 of the 3 TRP1/TCR mice originally imported from the National Cancer Institute that died. A single archived skin section from the ventrum was available and was reassessed under 100 to 200 $\times$  magnification. In addition, an attempt was made to rule out the possibility that the *Demodex* mites detected in TRP1/TCR mice originated from other mouse strains maintained by the same laboratory by examining archived skin from mice submitted to necropsy for 24 mo before and 12 mo after the TRP1/TCR mice arrived in quarantine. In addition, after *Demodex* mites were discovered, ectoparasite testing (including deep skin scrapes and fur plucks) was performed for mouse strains that were cohoused in the same animal holding rooms as the TRP1/TCR mice. Mice in 3 rooms were evaluated. The number of cages housed on ventilated racks (Thoren Caging Systems) in the 3 rooms ranged from 300 to 460 cages per room. One animal from a single cage from each row of each occupied rack was selected for ectoparasite testing. We evaluated 48 mice in room A, 64 mice in room B, and 22 mice in room C, representing 12%, 14%, and 7% of the cages in each room, respectively, and 40 different mouse lines and strains. Included in the testing were 4 dirty-bedding sentinel mice (Swiss Webster) from each room. Sentinel mice were exposed to soiled bedding from 40 cages on a weekly basis. For the epidemiologic assessment, ectoparasite tests were performed on live mice by trained veterinary technicians, and samples were analyzed by trained parasitology technicians.

In addition, 4 male and 4 female TRP1/TCR mice (The Jackson Laboratory) underwent fur plucks and deep skin scrapes immediately upon removal from the shipping container. As these mice aged, they were routinely observed for clinical signs related to the eyes and skin, and ectoparasite test samples were collected when clinical signs were noted.

**Statistical analyses.** Statistical analyses were performed using SAS version 9.4 (SAS Institute, Cary, NC). Summary statistics were generated. Population statistics comparing the effects of age and sex on the presence of clinical signs in TRP1/TCR mice were performed by using nonparametric tests (Wilcoxon rank sum test). For histologic topography of mites in TRP1/TCR skin, the percentage of follicles infested and the number of mites per millimeter of skin were compared among skin regions by using the Kruskal-Wallis test. To determine the anatomic sites with the highest numbers of mites, the median values of the mites per millimeter and the percentage of infested follicles were rank-ordered from highest to lowest for each region. The Spearman rank correlation coefficient was calculated to examine the degree of correlation between the values for the percentage of infested follicles and the number of mites per millimeter length of skin. *P* values less than 0.05 were considered significant.

## Results

**Clinical findings.** The initial animal evaluated was a 4-mo-old pregnant female parental TRP1/TCR mouse with exophthalmia and a body condition score of 2/5.<sup>88</sup> The left superior palpebra was ulcerated, and the left cornea was nonreflective and erythematous. Images of a mouse with a similar presentation are shown in Figure 1 A. An additional 47 parental strain mice from the colony were evaluated over the course of 1 y. Predominant clinical signs, when present, included pruritus, alopecia, UD, abscesses (especially retro- and periorbital), hunched posture, and an unkempt coat. Less common clinical signs included scaly dermatitis, poor body condition, skin pallor, and occasional soft stool. UD was identified as excoriation or ulceration of the skin that was associated with pruritus, typically of the face, ears, and cervical or interscapular regions.

Approximately half of the mice evaluated (26 of 48; 54.2%) presented with clinical signs. Clinically affected mice were significantly older (median age, 158 d; range, 56 to 852 d) than those without clinical signs (median, 85 d; range, 67 to 149 d; *P* = 0.0002). Almost half of the TRP1/TCR mice evaluated (23 of 48; 47.9%) presented with unkempt fur and pruritus. Nine animals (18.8%) had exophthalmia (Figure 1 A), and 9 had UD (18.8%; Figure 1 B). One mouse had skin pallor and an abnormal gait, and another mouse had a mass (1.5  $\times$  0.5 cm) on the right flank. A summary of clinical findings is presented in Table 1.

**Gross and microbiologic findings.** In addition to retroorbital abscesses, gross necropsy revealed suppurative inflammation or abscesses in other locations, including the middle and inner ear (*n* = 1), salivary gland (*n* = 1), inguinal lymph node (*n* = 1), and mammary gland and uterus (*n* = 2). Mice with UD had lesions on the face, neck, and one or both ears (*n* = 8) or the dorsum and legs (*n* = 1). One mouse had a hemoabdomen attributed to abdominal hemangiosarcoma, and a second had a hemoabdomen of undetermined cause. Bacterial cultures of suppurative lesions from the periocular tissue (*n* = 3), tympanic bulla (*n* = 1), and inguinal lymph node (*n* = 1) of TRP1/TCR mice were positive for *P. pneumotropica*. One sample cultured from a retroorbital abscess did not yield bacterial growth. In addition, 1 of 10 mice used for topography (see following) without clinical signs was found to have suppurative pneumonia, from which *P. pneumotropica* was isolated.

Culture samples taken from the skin of 4 mice with pruritus (a parental TRP1/TCR mouse with a retroorbital abscess and 3 reporter-strain mice with UD) were positive for *Corynebacterium bovis*. A summary of clinical, gross, histopathologic, and microbiologic findings from the additional mice evaluated are presented in Table 1.

**Microscopic findings.** In the mice with retroorbital abscesses whose tissues were evaluated microscopically (*n* = 3), moderate to severe, extensive, multifocal necrosis and suppurative inflammation were present in the periocular tissues, including the Harderian and parotid glands, subcutis, and maxillary skeletal muscles. Affected periocular tissues were infiltrated with large numbers of degenerate neutrophils admixed with cellular debris, fibrin, and coccobacilli, with moderate fibrosis (Figure 1 C). The coccobacilli were gram-negative (data not shown). In 2 female mice, multifocal necrosis was present in the endometrium and placenta, and the uterine lumen was infiltrated with large numbers of degenerate neutrophils admixed with coccobacillary bacteria.

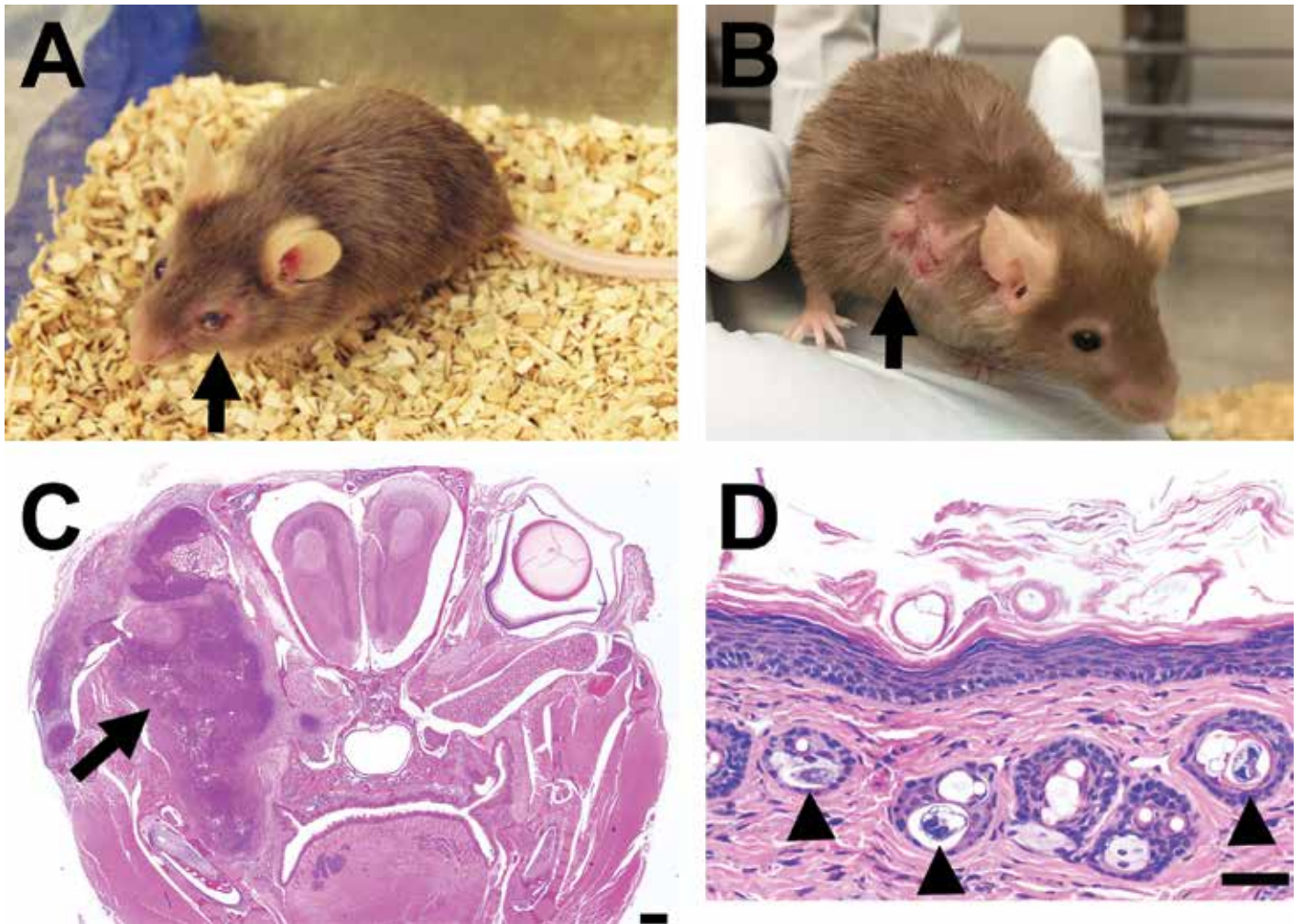


**Figure 1.** (A) Clinical presentation of a TRP1/TCR mouse with an unkempt coat and exophthalmia of the left eye (arrow). (B) A TRP1/TCR reporter-strain mouse with UD of the right shoulder (arrow). (C) Composite photomicrograph of a coronal section from a TRP1/TCR mouse with a retroorbital abscess (scale bar, 500  $\mu$ m). The image displays locally extensive multifocal necrosis and suppurative inflammation in the periocular tissues (arrow). (D) Orthokeratotic hyperkeratosis with acanthosis, epidermal hyperplasia, and intrafollicular mites (arrowheads) in the skin (low power; scale bar, 50  $\mu$ m). Note that the mites are not associated with inflammation.

In the skin, numerous follicular ostia and sebaceous glands contained elongated, cigar-shaped mites, consistent with *Demodex* spp. (Figure 1 D, arrowheads). Of the 9 mice necropsied, all had *Demodex* mites in the dermis and epidermis. When mites were present in the sebaceous glands, glands were often enlarged and dystrophic. Cellular infiltrates (neutrophilic or lymphocytic dermatitis) were present in the skin of 5 of the 9 necropsied mice and, although not associated with mites, were associated with coccobacilli with characteristic morphology of *C. bovis* in 2 of the 9 mice. Epidermal hyperplasia and acanthosis with mild, diffuse orthokeratotic hyperkeratosis was observed in the skin of most mice (Figure 1 D). All 9 mice had thymic, splenic, and lymph node depletion. Myeloid hyperplasia was noted in the lymph nodes, spleen, and bone marrow, consistent with neutrophilic infiltrates observed in the skin and other locations. Additional findings are summarized in Table 1.

**Parasitology and *Demodex* mite identification.** *Demodex* mites or eggs were present in the fur plucks and deep skin scrapes from 46 parental TRP1/TCR and 9 reporter-strain mice. Additional ectoparasite tests, such as superficial skin scrapes and

tape impression tests, were performed on most mice, but they were not as informative as were deep skin scrapes and fur plucks (data not shown). All (100%) of the 55 mice tested for ectoparasites were positive for *Demodex* mites on at least one test.

Parasite identification was performed on mites obtained from the skin fragment digestion method. The dimensions of the egg, immature mites (larva, protonymph, deutonymph), and adults (males and females) were recorded (Figure 2 and Table 2). The morphologic appearance and dimensions of the various life stages were consistent with *D. musculi*.<sup>28,39</sup>

**Topographic distribution of mites.** *Demodex* mites in histologic sections of dermis and epidermis from multiple skin regions (Figure 3 A) were counted. The number of mites in individual skin sections ranged from 0 to 42 (median, 4.2 mites). Across all skin sections, the percentage of follicles infested ranged from 0% to 21% (median, 2.7%). Whereas the ears and tail had no or few infested follicles (ears: median, 0%; range, 0% to 3.3%; tail: median, 0%, range 0% to 1.4%), the interscapular region (median, 8.1%; range, 2.0% to 16.6%), middorsum (median, 7.6%; range, 0% to 17%), and head (median, 4.9%; range, 2.3% to 21.1%) had

**Table 1.** Clinical signs, gross findings, histopathologic lesions, and microbiologic findings of 48 TRP1/TCR and 3 reporter-strain mice submitted for gross or complete necropsy

Sex	Age at necropsy (d)	Clinical signs at initial observation				Gross lesions			Histopathologic lesions					Microbiologic results <sup>f</sup>	
		Unkempt fur, pruritus	UD	Ocular lesion <sup>a</sup>	Hunched posture	Other <sup>b</sup>	Suppurative infection <sup>c</sup>	Other <sup>d</sup>	Dermatitis, folliculitis	Suppurative infection	Lymphoid depletion	Myeloid hyperplasia	Other <sup>e</sup>		
Parental strain															
F	133	+	-	+	+	-	+	+	-	+	+	+	+	+	NP
F	NA	+	-	+	-	-	+	+	+	+	+	+	+	+	Pp
F	322	+	-	+	+	-	+	+	+	-	+	+	-	None	
F	NA	-	-	-	+	+	+	+	-	+	+	+	+	+	Pp
F	773	+	-	-	+	+	+	+	+	+	+	+	+	+	NP
F	351	+	-	+	+	+	+	+	+	+	+	+	+	+	Pp, Cb
F	113	+	-	+	+	-	+	+	+	NP	-	-	-	+	Pp
F	NA	+	-	+	+	-	+	+	-	NP	NP	NP	NP	+	Pp
M	241	+	+	-	-	-	-	-	-	NP	NP	NP	NP	-	NP
F	260	+	+	-	-	-	-	-	-	NP	NP	NP	NP	-	NP
F	249	+	+	-	+	+	-	+	+	NP	NP	NP	NP	-	NP
M	291	-	-	-	-	+	-	+	-	NP	NP	NP	NP	-	NP
F	167	+	+	-	-	-	-	-	-	NP	NP	NP	NP	-	NP
M	106	-	-	-	-	-	-	-	-	NP	NP	NP	NP	-	NP
F	388	+	+	-	+	-	-	-	-	NP	NP	NP	NP	-	NP
F	120	+	-	+	+	-	-	-	-	NP	NP	NP	NP	-	NP
M	130	+	-	+	-	+	-	+	-	NP	NP	NP	NP	-	NP
M	852	+	+	-	-	-	-	-	-	NP	NP	NP	NP	-	NP
M	56	+	-	+	+	+	-	+	+	NP	NP	NP	NP	-	NP
F	85	+	-	+	-	+	-	+	-	NP	NP	NP	NP	-	NP
F	496	+	+	-	+	+	-	+	+	NP	NP	NP	NP	-	NP
F	91	+	+	-	+	+	-	+	+	NP	NP	NP	NP	-	NP
M	149	+	-	+	+	+	-	+	-	NP	NP	NP	NP	-	NP
M	149	+	-	-	-	-	-	-	-	NP	NP	NP	NP	-	NP
M	149	+	-	-	-	-	-	-	-	NP	NP	NP	NP	-	NP
M	85	+	-	-	-	-	-	-	-	NP	NP	NP	NP	-	NP
12M	85	-	-	-	-	-	-	-	-	NP	NP	NP	NP	-	NP
10F	(67-149)														

Reporter strains

M	522	+	+	-	-	+	-	+	+	NP	+	+	+	+	Cb
F	285	+	+	-	-	-	-	-	-	+	+	+	+	+	Cb
F	285	+	+	-	-	-	-	-	-	+	+	+	+	+	Cb

Cb, *Corynebacterium bovis*; F, female; M, male; NA, not available; NP, not performed; Pp, *Pasteurella pneumotropica*; UD, ulcerative dermatitis

<sup>a</sup>Includes retroorbital abscesses, corneal abrasion, and corneal ulceration

<sup>b</sup>Includes scaling dermatitis, poor body condition, skin pallor, soft stool, and rectal prolapse

<sup>c</sup>Includes retroorbital abscess; otitis media or interna; mastitis; pyometra; or abscesses in lymph nodes, clitoral glands, or preputial glands

<sup>d</sup>Includes pregnancy, hemoabdomen, mass effects, splenomegaly, lymphadenopathy, tissue cysts (renal, adrenal, or salivary gland), edema or tissue ulceration

<sup>e</sup>Includes extramedullary hematopoiesis; gastrointestinal inflammation and necrosis (colitis); neutrophilic periodontitis with intralesional hair shafts; renal interstitial fibrosis and mineralization; hydronephrosis; ovarian atrophy; neoplasia; periportal hepatitis

<sup>f</sup>Samples from suppurative exudates and skin were submitted for aerobic culture

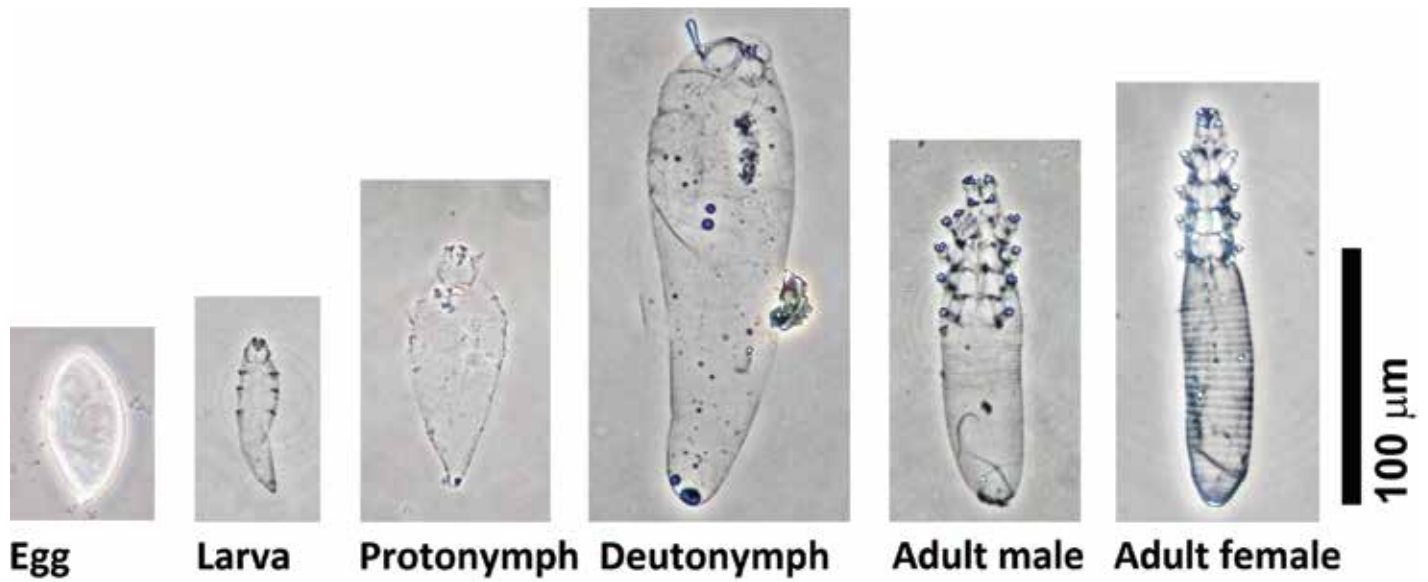


**Figure 2.** The appearance of various life stages of *Demodex musculi* isolated by using the skin fragmentation digestion method. Scale bar, 100 μm.

**Table 2.** The dimensions of various life stages of *Demodex musculi* found in the pelts of 4 TRP1/TCR mice

Life stage (n)	Length (μm)		width (μm)	
	Mean ± SEM	Range	Mean ± SEM	Range
Eggs (52)	34.6 ± 0.6	25–45	15.2 ± 0.4	10–21
Larvae (100)	60.3 ± 0.8	44–75	17.8 ± 0.2	13–23
Protonymphs (100)	87.1 ± 1	68–121	26.9 ± 0.5	20–45
Deutonymphs (100)	163.4 ± 2.6	114–203	50.1 ± 0.5	38–60
Adult males (100)	138.1 ± 1.0	118–158	33.2 ± 0.3	23–41
Adult females (100)	159.3 ± 1.0	135–193	34.6 ± 0.2	29–46

the highest percentages of infested follicles when rank ordered by median (Figure 3 B and C). The number of mites per millimeter of skin ranged from 0 to 3.7 (median, 0.5 mites) across all mice tested. In general, the number of mites per millimeter of skin mirrored that of the percentage of follicles infested (Figure 3 B and C) by region, but the primary rank order indicated that the middorsum (median, 1.2; range, 0 to 2.8), interscapular region (median, 1.0; range 0.3 to 2.0), and caudal dorsum (median, 0.9; range 0.2 to 2.0) had the highest median number of mites per millimeter of skin. There were significant differences in both the percentage of infested follicles and number of mites per millimeter of skin when all skin regions were compared ( $P < 0.0001$  [Kruskal–Wallis test]; Figure 3 B and C). The values for percentage of follicles infested and number of mites per millimeter were compared. The positive Spearman rank coefficient for the compared values was 0.97 ( $P < 0.001$ ) when values from all regions were included, indicating a strong correlation.

Microscopically, mite appearance was highly variable depending on life stage and the specific anatomic region in the mite section. The anatomic regions identified included the gnathosoma, containing the mouth parts, chelicerae, and palpi; the podosoma, the cranial region bearing the legs; and the opisthosoma, the caudal region containing internal organs (Figure 4 A and B).<sup>15</sup> In section, the gnathosoma appeared highly eosinophilic, simi-

lar in appearance to keratin (Figure 4 C and D). Sections of the podosoma were wider than those of the gnathosoma and were also eosinophilic, but contained basophilic skeletal muscle cell nuclei (Figure 4 E through H). The opisthosoma was highly variable depending on whether the mite was male or female and on whether the section included reproductive structures (ovary, egg, or testis), skeletal muscle, the synganglion, or gut cells (Figure 4 I through M). Mite eggs appeared densely basophilic due to aggregates of nuclei (Figure 4 N [longitudinal] and O [transverse]). Luna staining did not enhance mite identification, and normal skin structures demonstrated nonspecific staining (not shown).

**Epidemiologic investigation of mite source.** A retrospective histologic assessment was performed in an attempt to identify the mite source. The single skin section from a single mouse imported from the National Cancer Institute was available for analysis and was negative for *Demodex* mites. We did not find histologic evidence of *Demodex* mites in epidermis from skin sections of multiple mice (including the head, ears, and tail) that had been submitted for analysis by the investigator for experimental use before and after the infestation was identified; however, only 38 archival skin sections were available for analysis.

In addition, after *Demodex* mites were discovered, ectoparasite testing was conducted on mouse strains housed in the same 3 animal holding rooms as the TRP1/TCR mice. In 2 of the 3

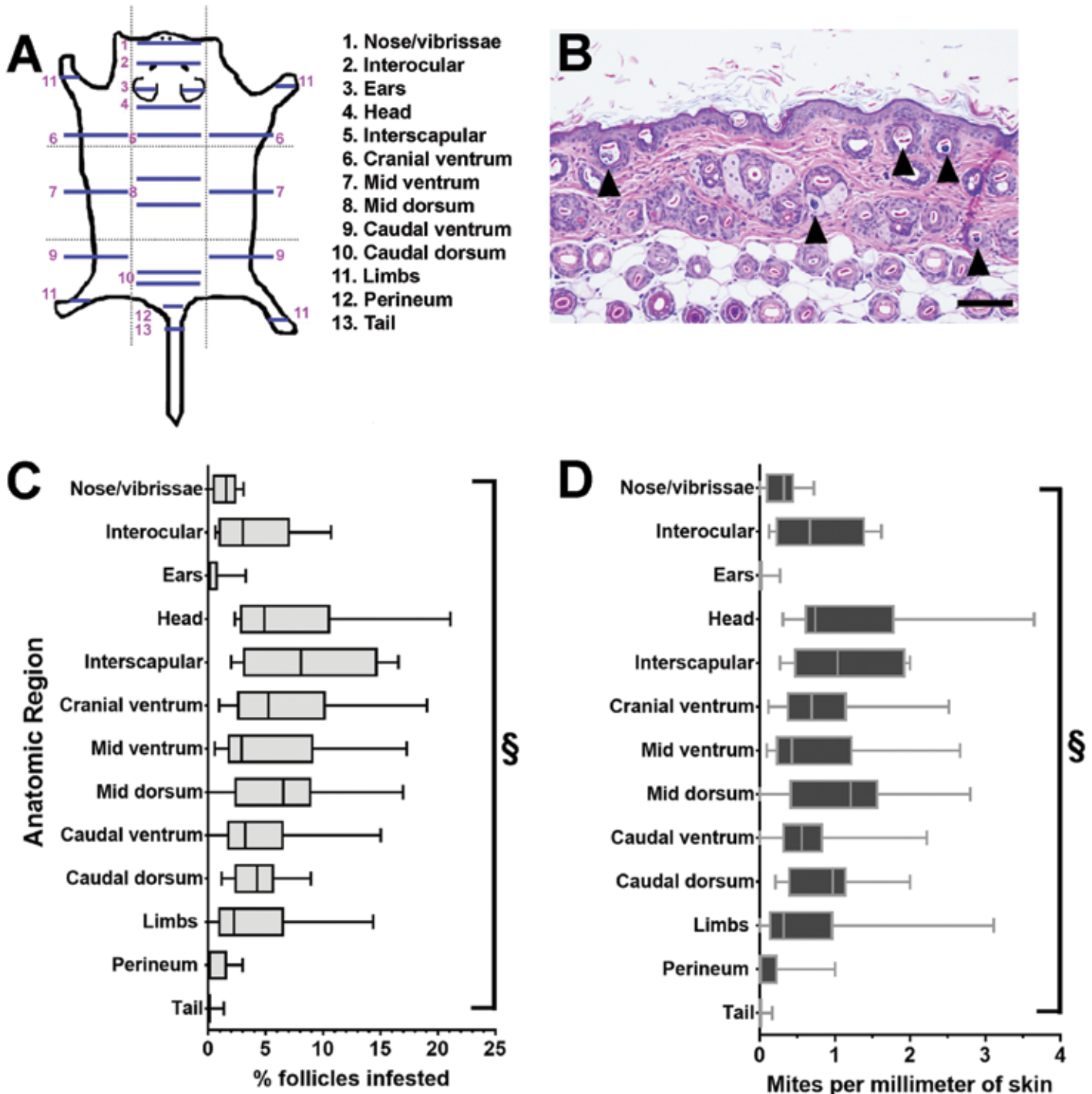


**Figure 3.** In total, 22 skin sections from 13 skin regions of TRP1/TCR mice were analyzed for *Demodex* mites. (A) The numbers of mites and follicular cross sections were counted in the epidermis and dermis (see Figure 1 D for an example). (B) The percentage of infested follicles was calculated by dividing the number of mites by the number of follicular cross sections evaluated. (C) The number of mites per millimeter was calculated by dividing the number of mites by the length of the skin sections in millimeters. The data are displayed as the median (central line), with the first and third quartiles indicated by the boxes and the upper and lower limits of the ranges bounded by the whiskers. The anatomic regions differed significantly regarding both the percentage of follicles infested and the number of mites per millimeter (§,  $P < 0.0001$ ; Kruskal–Wallis test).

rooms, only TRP1/TCR parental and reporter-line mice, used as positive controls, were found to be infested. In the third room, 2 other strains were found to have *Demodex* mites. For each of the 2 mouse strains, 3 of 5 (60%) of the mice tested were posi-

tive for *Demodex* mites on ectoparasite testing. These 2 strains were mouse models of melanoma (Pmel–Thy1.1 and Grm1–TG3 mice) and had not previously been crossed with TRP1/TCR mice. The exact genotypes of the melanoma models were not avail-



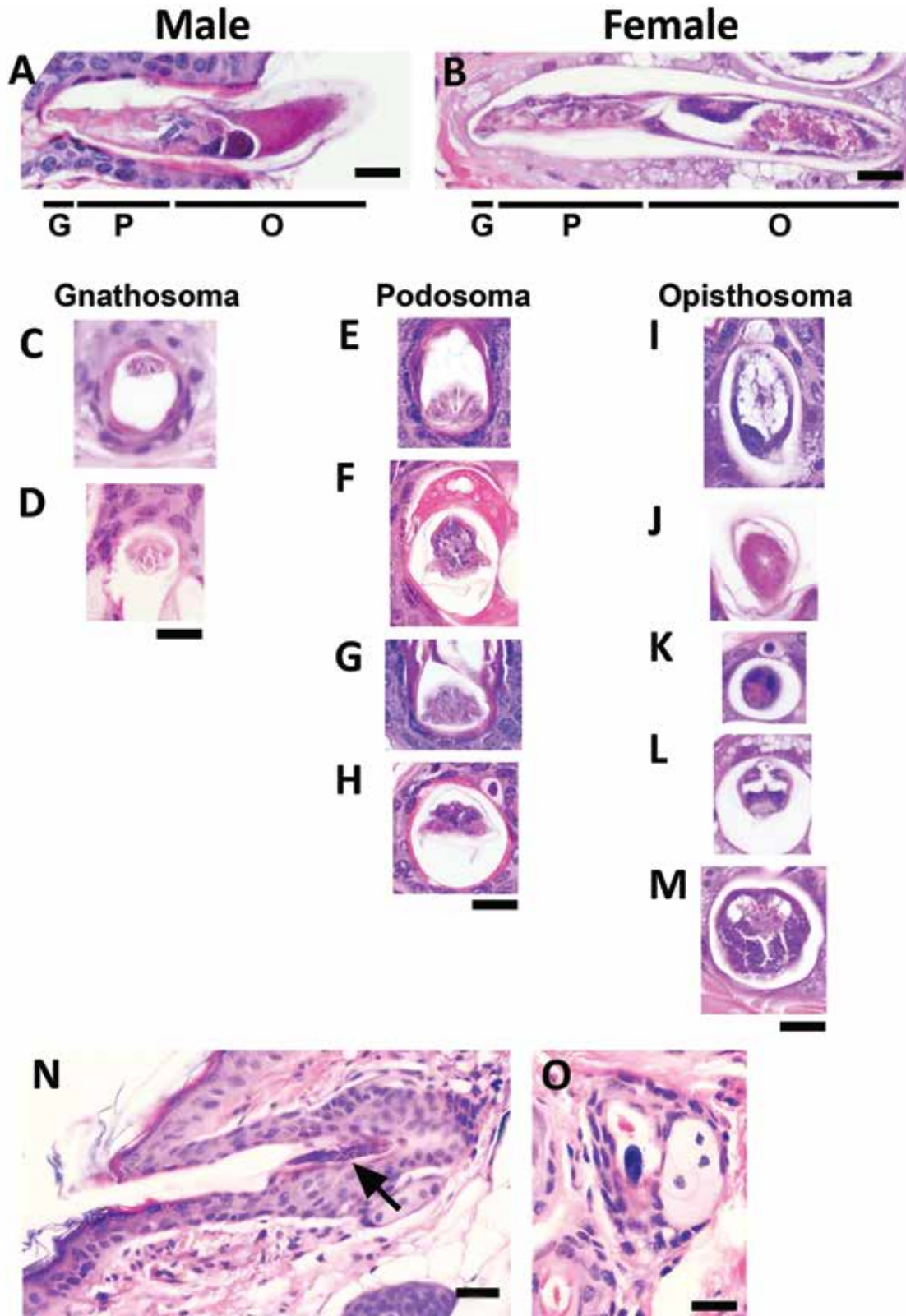


**Figure 4.** Longitudinal and transverse sections of mites observed during topographic analysis of TRP1/TCR mouse skin sections. The diversity in appearance of mites is shown with representative images of *Demodex* mites viewed under high magnification (600×). The body segments in (A) male and (B) female mites include the gnathosoma (mouth parts [G]), podosoma (cranial region with legs [P]), and opisthosoma (caudal region [O]). Male and female mites differ in length and reproductive structures. Transverse sections of the (C and D) gnathosoma, (E–H) podosoma, and (I–M) opisthosoma are shown. Mite eggs (N, longitudinal; O, transverse) appear as dark basophilic structures. Scale bar, 20 μm (A–M, O); 30 μm (N).

able, but given the strain names, they are likely B6.Cg-Thy1<sup>a</sup>/CyTg(TcraTcrb)8Rest and C57BL/6-Tg(Grm1)EPv, respectively. These mouse strains are not known to be inherently immunodeficient. In addition, dirty-bedding sentinel mice from each of the 3 rooms were ectoparasite-tested. One sentinel mouse in the smallest, most heavily infested room had a single dead mite. Because the source could have been the transferred bedding, the mouse was euthanized, and the skin was evaluated microscopically. Histologic assessment revealed 2 follicular mites in the mouse's facial skin. Subsequent ectoparasite testing and histology of sentinel mice from the 3 rooms did not yield further infestation with *Demodex* mites.

All 8 TRP1/TCR mice that were purchased from The Jackson Laboratory and tested on arrival were negative for *Demodex* mites by fur pluck and deep skin scrape. As the mice aged, they displayed unkempt appearance and had minor eye lesions. Mites were never detected on ectoparasite tests, and aerobic culture of the skin from the 5 mice evaluated were negative for *C. bovis* (data not shown).

**Case resolution.** In light of the assumption that all or at least the majority of suppurative lesions in this mouse strain were associated with *P. pneumotropica* infection, the breeding colony was placed prophylactically on laboratory rodent chow supplemented with amoxicillin (0.12% amoxicillin; Purina TestDiets), and the number of clinical cases decreased dramatically. Occasional treatment-refractory cases of UD continue to be present in the TRP1/TCR colony.

Although the research implications and transmissibility of *Demodex* mites had not been completely characterized, additional requirements regarding personal protective equipment were instituted in rooms housing TRP1/TCR mice and related strains with *Demodex* mites because the facility has a large number of immunocompromised mouse strains that are used for oncology research. These additional requirements stipulated a secondary disposable gown, shoe covers, and a standard surgical mask; these items are doffed on exit from the holding room. In addition, treatment options for *Demodex* mites were discussed with the principal investigator.

## Discussion

This report demonstrates that *D. musculi* mites can be present in immunocompromised laboratory mice maintained under SPF conditions. Although *Demodex* mites have rarely been identified in laboratory mice, they are likely underrecognized. Of the few descriptions of *Demodex* infestations in laboratory mice, the most severely affected mouse strains had an underlying immunodeficiency, which likely facilitated mite detection.<sup>27,50,85</sup>

TRP1/TCR mice are commercially available from The Jackson Laboratory. This strain contains the *Rag1*<sup>tm1Mom</sup> targeted mutation, which deletes the RAG1 enzyme required for V(D)J recombination in the normal development of lymphocytes.<sup>57,62</sup> Therefore, these mice lack normal mature T and B lymphocyte morphology and function and have abnormal adaptive immunity. In TRP1/TCR mice, although the white-based brown mutation (*Tyrp1*<sup>B-w</sup>) affects melanocytes and the Y-chromosome-based transgene yields T cells that target melanocytes (Tg(Tcra,Tcrb)9Rest), we do not expect these components of the genotype to significantly influence the strain's susceptibility to opportunistic bacteria and *Demodex* mites.

*Rag1*-null mice have been studied extensively, and they respond abnormally when exposed to infectious agents.<sup>4,47,57</sup> Potential etiologies of suppurative inflammation of multiple organs that resulted in the clinical signs in TRP1/TCR mice include *P. pneumotropica*, *Staphylococcus* spp., *Streptococcus* spp., *Klebsiella* spp., *Corynebacterium* spp., and *Mycoplasma* spp.<sup>67,70</sup> *P. pneumotropica* is a common commensal of mucosal surfaces, but it is considered an opportunistic pathogen in immunodeficient mouse strains.<sup>3,25,46,58</sup> *C. bovis* causes hyperkeratosis and scaly dermatitis in mice, especially those with defective adaptive immunity.<sup>80,81</sup> *P. pneumotropica* and *C. bovis* were known to be enzootic in mice housed in our vivaria and were readily cultured, but the presence of *Demodex* mites was unexpected.<sup>11</sup> Had we forgone investigation of the ocular and skin lesions in TRP1/TCR mice with histology and ectoparasite testing, the *Demodex* mites may have remained undetected. As indicated in published literature, we first noted *Demodex* mites in TRP1/TCR mice histologically, and we and others have also detected mites in ectoparasite tests (fur plucks and deep skin scrapes).<sup>27,50,85</sup>

The mites isolated from the TRP1/TCR mice were consistent with descriptions of *D. musculi*, the only demodicid mite reported in laboratory mice thus far.<sup>27,28,39,50,85</sup> To our knowledge, this study is the first to demonstrate all life stages of *D. musculi*, including the immature stages (egg, larva, protonymph, and deutonymph), in laboratory mice.<sup>28,39</sup> There are 8 genera of known demodicid mites affecting 12 orders of placental and marsupial mammals.<sup>40</sup> Species identification of demodicid parasites is generally performed morphometrically after the skin fragmentation digestion technique, with a focus on the mite's body length and width, the shape and appearance of anatomic structures such as the palps and supracoxal spines of the gnathosoma, and the configuration of the tarsal claws.<sup>15,23,32</sup> *Demodex* mites are generally host-specific, but multiple mite species can infect a single host.<sup>79</sup> Until recently, only 2 species of *Demodex* mites have been isolated from wild *Mus musculus*: *D. musculi* and *D. flagellurus*.<sup>8,9,28</sup> *D. flagellurus* is found in the preputial and clitoral glands and is transmitted both by sexual and direct contact.<sup>9</sup> In other species, for example, grasshopper mice (*Onychomys leucogaster*), striped field mice (*Apodemus agrarius*), and European wood mice (*A. sylvaticus*), demodicid mites have been isolated from the oral cavity (esophagus and tongue), Meibomian glands, and ear canal.<sup>10,36,51,64</sup> Reevaluation of wild European *Mus musculus musculus* has recently led to the identification of additional demodicid species, including *D. fusiformis*, *D. marculus*, *D. conicus*, and *D. vibrissae*, in the skin, including vibrissae follicles and ear canals.<sup>38,39,41</sup> Recently a novel demodicid mite, *Glossicodex musculi*, was observed in the tongue of wild *Mus musculus musculus*.<sup>40</sup> Mites in the oral cavity are presumably transmitted via grooming and have evolved to adapt to that niche.<sup>64</sup>

*Demodex* infestation in immunosuppressed animals may cause hyperkeratosis with scaling, pruritus, erythema, comedones or nodules; alopecia; UD; and regional lymphadenopathy.<sup>43,61,86</sup> In addition, significant mite burdens damage the protective skin barrier in mammals and may predispose animals to secondary infections with commensal skin or gut flora.<sup>24,61,63</sup> It is conceivable that *D. musculi* infestation facilitated the proliferation and potentially the invasiveness of the opportunistic bacterial pathogens in our TRP1/TCR mice. Prior reports of *D. musculi* infestation in mice presenting with clinical signs did not describe culture of the skin, so whether additional opportunistic agents contributed to the clinical manifestations in those cases is unclear.<sup>50,85</sup> Why the

TRP1/TCR mice did not display clinical signs until after the colony was moved from the breeding facility to the experimental facility is unknown. Sentinel mice (Swiss Webster stock) from both the breeding and experimental barrier facilities tested positive for *P. pneumotropica* and *C. bovis* (data not shown). One possibility is that TRP1/TCR mice were exposed and infested with *Demodex* upon transfer to the experimental facility. Additional studies are required to better understand *Demodex* mite prevalence and transmission in laboratory mice. We cannot rule out the possibility that transport stress played a role in the disease course. The contribution of background strain to *Demodex* susceptibility is uncertain as well. In addition to mice on a C57BL/6 background, mice on a BALB/c background have been reported with *Demodex* mites.<sup>50,85</sup>

Although fur mites have been associated with pruritus and UD in the literature, it is unclear whether murine demodicosis is pruritic.<sup>16,17,60</sup> In other species, uncomplicated *Demodex* mite infestations may or may not cause pruritus.<sup>54,59,77,82,86</sup> In TRP1/TCR mice, the pruritus may have been secondary to the *Corynebacterium*-associated hyperkeratosis and *Pasteurella* otitis, resulting in self-trauma and UD as sequelae. Treatment with amoxicillin eliminated *P. pneumotropica*- and *Corynebacterium*-associated infections and greatly reduced pruritus and the incidence of UD, although the mites remained present. Occasional cases of UD, refractory to treatment, are still observed in the TRP1/TCR colony; thus, we suspect that *Demodex* mites contribute to pruritus in mice. In addition, the UD may have a genetic basis due to the C57BL/6 contribution to the TRP1/TCR genotype. Interestingly, of the 9 mice with UD in this report, the skin lesions were predominately on the face and ears (8 of the 9 mice). It is plausible that these mice had otitis, prompting scratching of the head and ears, but complete necropsies were not performed on all mice with UD.

Younger TRP1/TCR mice were less likely to display clinical signs related to opportunistic infections. This pattern could be a function of age, which is a known risk factor, but we cannot rule out the contribution of mites.<sup>7</sup> Presumably, younger animals have fewer follicular mites, and mites continue to replicate over time due to the lack of adaptive immunity, occupying an increasing numbers of follicles over time. With murine fur mites, such as *Myocoptes musculus*, mite populations peak at earlier ages and then decline over time; however in *Rag1*-null mice, the mite burden increases with age.<sup>56,74</sup> The continued presence of mites also may result in stress, which can contribute to morbidity.

In TRP1/TCR mice, *D. musculi* was found in most areas of skin except the tail and most of the pinnae, reflecting a generalized demodicosis. Although localized compared with generalized demodicosis has not been defined in rodents, in species such as dogs, a localized infestation involves one to several circumscribed lesions attributed to *Demodex* mite parasites, whereas a generalized infestation refers to affected skin on more than 50% of the body.<sup>61</sup> The distribution of mites in mice may determine the best anatomic sites for diagnostic testing and inform selection of potential treatment routes. The tail and ears may not be preferred sites for *D. musculi* because the hair density is lower (possibly inhibiting follicle-to-follicle transfer), and the follicular ostia have a wider diameter in the tail compared with those found in other areas of skin. In contrast, in rats (*Rattus norvegicus*), *Demodex* mites have adapted to sparsely haired skin.<sup>37</sup>

Topographically, differences in the medians of the percentage of infested follicles and the number of mites per millimeter were possibly due to differences in the density of follicles in various an-

atomic regions. In the 10 mice evaluated, as many as 21.1% of follicles were infested in a single region, and each follicle had between 1 to 3 mites or eggs. In other species, such as dogs and humans, the number of mites per follicle ranges from one to numerous mites.<sup>14,15,29,75</sup> In light of the higher percentage of follicles infested in the head, interscapular region, and middorsum of TRP1/TCR mice, these sites may be ideal for antemortem skin sampling. Other studies in mice sampled the head and neck regions for *Demodex* mites by using fur plucks.<sup>27,85</sup> Assessing whether *D. musculi* has a different topographic preference in other laboratory mouse strains, especially immunocompetent stocks and strains, would be valuable. In one report, *D. musculi* was present in 81% of wild European *Mus musculus musculus* examined, and the distribution mirrored what we observed in TRP1/TCR mice: mites were observed in the head, neck, abdomen, back, limbs, and anogenital area.<sup>39</sup> Other mite species, such as fur mites, and *Demodex* mites in other rodents have more limited topographic preferences.<sup>32,33,36,48</sup>

*D. musculi* was observed in the dermis and epidermis, but not the subcutis. When mites were viewed in section, they were readily observed when the section included the opisthosoma, but visualization of mites sectioned through the gnathosoma and podosoma was more difficult because the eosinophilic appearance of the chitinous exoskeleton and mite skeletal muscle resembled keratin. Higher magnification was used to confirm the presence of small punctate basophilic nuclei, which aided in mite identification. Likewise, the appearance of sectioned mite eggs with their small cell nuclei had to be verified under higher magnification (400×), because they could be mistaken for mast cells with prominent basophilic granules, which are common in mouse dermis. We speculate that in immunocompetent animals with a low burden of follicular mites, it is possible to overlook *Demodex* mites or eggs when skin sections are viewed under low magnification. This situation may contribute to an underreporting of *Demodex* in laboratory mice.

In addition to the difficulty in detecting the mites microscopically, we suspect other reasons contribute to why *Demodex* mites are rarely detected. First, ectoparasites likely are not present in mice that have been rederived, such as those sourced from commercial vendors. Second, in immunocompetent animals, mites are likely present at low levels and are difficult to detect without rigorous skin sampling.<sup>27</sup> Histology is a useful tool to detect *Demodex* mites, but an exhaustive examination of various skin regions (as done during the topographic analysis in the current report) is not typically conducted and is highly labor-intensive. Finally, standard methods of detection of other ectoparasites are not sufficiently sensitive to detect follicular mites. Because TRP1/TCR mice have moderate numbers of *D. musculi*, detecting mites microscopically in skin sections and on ectoparasite tests was relatively easy. Further research into the best antemortem diagnostics for detection of *D. musculi* is warranted. Surface-dwelling mites, such as fur mites, can readily be detected by using PCR analysis, and evidence suggests that PCR assays can also be used for the detection of burrowing mites.<sup>2,44,74</sup> Recent unpublished work in our laboratory suggests that molecular diagnostics can effectively detect *Demodex* mites in laboratory mice.

The origin of the mites in the TRP1/TCR mice remains obscure. Direct contact is the most common mode of transmission for follicular mites.<sup>27</sup> Although wild mice carry *D. musculi*,<sup>28,39</sup> it is highly unlikely that they were a source of the infestation, because there was no evidence of an incursion in the facilities in which the mice

were housed and, even had an incursion occurred, the caging system and practices used in our facilities would make it almost impossible for direct contact to occur. Ectoparasite testing of non-TRP1/TCR mouse strains housed in the same animal holding room as the TRP1/TCR mice revealed 2 *Demodex*-positive strains. Whether either of these presumed immunocompetent strains was responsible for infesting the TRP1/TCR colony or vice versa is unclear. These strains might have been independently infested, but because they were present in the holding room with the highest mite burden, we suspect that TRP1/TCR mice were the source of the mites for those strains. The single sentinel mouse with its small number of mites suggests that dirty bedding could potentially be a fomite for *Demodex* mites, but rigorous assessment of fomite transmission of follicular mites has not been assessed in rodents. Since recognizing *Demodex* mites in our vivarium, we increased the intensity of surveillance for mites in mice imported from other institutions. After a PCR assay for *Demodex* became commercially available, we have confirmed that *Demodex* mites are present in other mice in our vivaria and in several of our murine imports (13% of the strains imported from 120 institutions were found to be infested).<sup>73</sup> In most of these cases, *Demodex* infestation is subclinical. If fomite transmission is possible, TRP1/TCR mice might have been infested on transfer from the breeding facility to the experimental facility, despite our high level of biosecurity practices.

Mammals have long been colonized with *Demodex* mites, which may partially explain immune tolerance to the mite in healthy subjects.<sup>22,66,85</sup> *Demodex* mite transmission from dam to offspring, the life cycle, and its biology may play roles in immune tolerance. For example, the inability of *Demodex* mites to produce fecal waste, because they have a blind-ended gut with no anus, may make them less immunogenic than other mites.<sup>20,55</sup> The adaptive immunodeficiency in TRP1/TCR mice made them permissive to *Demodex* infestation, but information about host immune responses to *Demodex* is limited.<sup>1,22,24,85</sup> Mature T cells, absent in TRP1/TCR mice, are important in the immune response against both *Demodex* and bacterial dermatitis, but because of complex immune abnormalities in *Rag1*-null mice, including lack of mature B cells, we cannot confirm whether T cells alone are responsible for the susceptibility of TRP1/TCR mice to the mite.<sup>27,85</sup> Immunity against other mite species such as *Sarcoptes scabiei*, *Myocoptes musculinus*, and *Psoroptes ovis* indicate that both innate and adaptive immune responses are important.<sup>12,56,78,89,90</sup>

We surmise that TRP1/TCR mice have some sort of immune response to *Demodex* mites, because they had few mites per follicle, and only moderate numbers of follicles were infested. Which innate responses contribute to immunity in RAG1-deficient mice is unknown, but eosinophils, mast cells, dendritic cells, NK cells, and macrophages all may contribute to host immunity. In addition, keratinocytes or antimicrobial peptides may be involved in the recognition and control of ectoparasites with chitinous exoskeletons.<sup>45</sup> In contrast to TRP1/TCR mice, a *Rag2*-null strain and mice lacking IL-13, a cytokine important in the Th2 response, were reported to have high numbers of *Demodex* mites.<sup>85</sup> Although Th2 responses are clearly involved, the RAG2-deficient strain also lacked functional NK cells, due to a null mutation of IL2R $\gamma$ .<sup>85</sup> NK cells may be a key factor in host defense against mites.

In dogs, abnormalities in T-cell function are implicated in the pathogenesis of generalized demodicosis.<sup>22</sup> In humans, *Demodex* mites have been associated with a type IV hypersensitivity reac-

tion with Th2-based lymphocytic infiltrates and phagocytosis of mites by macrophages.<sup>24,76</sup> Although mixed inflammation has been observed associated with *Demodex* mites and debris in both humans and mice, infiltrates associated with infested follicles in TRP1/TCR mice were not apparent,<sup>29,50</sup> likely due to the immune suppression of these mice.

Because increases in mite density have been correlated with clinical signs in humans,<sup>21,23,83</sup> *Rag1*-null mice may represent a valuable model for human dermatologic and ocular conditions and for canine generalized demodicosis with regard to host immunity, comorbidities, and potential therapies. In addition, because immunocompromised mouse models are widely used for immunologic and cancer research, it is important to consider *Demodex* mites in the etiology of unexplained cases of skin disease, and a thorough diagnostic workup, including skin culture, fur pluck, deep skin scrape, PCR analysis, and necropsy with histopathology should be performed to increase the likelihood of detecting opportunistic bacteria and ectoparasites. We have embarked on further studies examining diagnostics for and treatment of murine demodicosis. The effect of *Demodex* mites on the immune system and their potential as an experimental variable should be investigated also, because the mites have the potential to influence research results.

---

## Acknowledgments

We thank the members of Dr Taha Merghoub's laboratory, especially Hong Zong, for their cooperation. The staffs of the Center of Comparative Medicine, Laboratory of Comparative Pathology (especially Jacqueline Candelier), and Veterinary Services provided assistance with this project. We appreciate the help of Dr Felix Wolf, who assisted with the epidemiological investigation, and Souci Louis, who performed retrospective histologic analysis. This work was supported in part by a Core Grant from the National Cancer Institute (P30 CA 008748) to the Memorial Sloan Kettering Cancer Center.

---

## References

1. Akilov OE, Mumcuoglu KY. 2004. Immune response in demodicosis. *J Eur Acad Dermatol Venereol* 18:440-444.
2. Angelone-Alasaad S, Molinar Min A, Pasquetti M, Alagaili AN, D'Amelio S, Berrilli F, Obanda V, Gebely MA, Soriguer RC, Rossi L. 2015. Universal conventional and real-time PCR diagnosis tools for *Sarcoptes scabiei*. *Parasit Vectors* 8:1-7.
3. Artwohl JE, Flynn JC, Bunte RM, Angen O, Herold KC. 2000. Outbreak of *Pasteurella pneumotropica* in a closed colony of STOCK-Cd28(tm1Mak) mice. *Contemp Top Lab Anim Sci* 39:39-41.
4. Aurora AB, Baluk P, Zhang D, Sidhu SS, Dolganov GM, Basbaum C, McDonald DM, Killeen N. 2005. Immune complex-dependent remodeling of the airway vasculature in response to a chronic bacterial infection. *J Immunol* 175:6319-6326.
5. American Veterinary Medical Association. 2013. American Veterinary Medical Association guidelines for the euthanasia of animals. Schaumburg (IL): American Veterinary Medical Association.
6. Bochkov AV. 2008. New observations on phylogeny of Cheyletoid mites (*Acari: Prostigmata; Cheyletoidea*). *Proceedings of the Zoological Institute* 312:54-73.
7. Brayton CF, Treuting PM, Ward JM. 2012. Pathobiology of aging mice and GEM: background strains and experimental design. *Vet Pathol* 49:85-105.
8. Bukva V. 1985. *Demodex flagellurus* sp. n. (Acari: Demodicidae) from the preputial and clitoral glands of the house mouse, *Mus musculus* L. *Folia Parasitol (Praha)* 32:73-81.

9. Bukva V. 1990. Transmission of *Demodex flagellurus* (Acari: Demodicidae) in the house mouse, *Mus musculus*, under laboratory conditions. *Exp Appl Acarol* **10**:53–60.
10. Bukva V. 1994. *Demodex agrarii* sp. n. (Acari: Demodicidae) from cerumen and the sebaceous glands in the ears of the striped field mouse, *Apodemus agrarius* (Rodentia). *Folia Parasitol (Praha)* **41**:305–311.
11. Burr HN, Lipman NS, White JR, Zheng J, Wolf FR. 2011. Strategies to prevent, treat, and provoke *Corynebacterium*-associated hyperkeratosis in athymic nude mice. *J Am Assoc Lab Anim Sci* **50**:378–388.
12. Casais R, Dalton KP, Millan J, Balseiro A, Oleaga A, Solano P, Goyache F, Prieto JM, Parra F. 2014. Primary and secondary experimental infestation of rabbits (*Oryctolagus cuniculus*) with *Sarcoptes scabiei* from a wild rabbit: factors determining resistance to reinfestation. *Vet Parasitol* **203**:173–183.
13. Caswell JL, Yager JA, Barta JR, Parker W. 1996. Establishment of *Demodex canis* on canine skin engrafted onto SCID-beige mice. *J Parasitol* **82**:911–915.
14. Caswell JL, Yager JA, Parker WM, Moore PF. 1997. A prospective study of the immunophenotype and temporal changes in the histologic lesions of canine demodicosis. *Vet Pathol* **34**:279–287.
15. Cribier B. 2013. Rosacea under the microscope: characteristic histological findings. *J Eur Acad Dermatol Venereol* **27**:1336–1343.
16. Csiza CK, McMartin DN. 1976. Apparent acaridal dermatitis in a C57BL/6 Nya mouse colony. *Lab Anim Sci* **26**:781–787.
17. Dawson DV, Whitmore SP, Bresnahan JF. 1986. Genetic control of susceptibility to mite-associated ulcerative dermatitis. *Lab Anim Sci* **36**:262–267.
18. Desch CE, Hurley RJ. 1997. *Demodex sinocricetuli*: new species of hair follicle mite (Acari: Demodicidae) from the Chinese form of the striped hamster, *Cricetulus barabensis* (Rodentia: Muridae). *J Med Entomol* **34**:317–320.
19. Desch CE Jr. 1989. The digestive system of *Demodex folliculorum* (Acari: Demodicidae) of man: A light and electron microscope study, p 187–195. In: Channabasavanna GP, Viraktamath CA, editors. *Progress in Acarology*, vol 1. Leiden (Netherlands): EJ Brill.
20. Desch CE, Nutting WB. 1978. Morphology and functional anatomy of *Demodex folliculorum* (Simon) of man. *Acarologia* **19**:422–462.
21. el-Bassiouni SO, Ahmed JA, Younis AI, Ismail MA, Saadawi AN, Bassiouni SO. 2005. A study on *Demodex folliculorum* mite density and immune response in patients with facial dermatoses. *J Egypt Soc Parasitol* **35**:899–910.
22. Ferrer L, Ravera I, Silbermayr K. 2014. Immunology and pathogenesis of canine demodicosis. *Vet Dermatol* **25**:427–e65.
23. Forton F, Seys B. 1993. Density of *Demodex folliculorum* in rosacea: a case-control study using standardized skin-surface biopsy. *Br J Dermatol* **128**:650–659.
24. Forton FM. 2011. Papulopustular rosacea, skin immunity and *Demodex*: pityriasis folliculorum as a missing link. *J Eur Acad Dermatol Venereol* **26**:19–28.
25. Franklin CL. 2006. Microbial considerations in genetically engineered mouse research. *ILAR J* **47**:141–155.
26. Gressler LT, Schafer da Silva A, Sessegolo T, Bürguer ME, Gonzalez Monteiro S. 2010. Ivermectina no tratamento de camundongos (*Mus musculus*) infestados por ácaros. *Acta Sci Vet* **38**:47–50 [Article in Portuguese].
27. Hill LR, Kille PS, Weiss DA, Craig TM, Coghlan LG. 1999. *Demodex musculi* in the skin of transgenic mice. *Contemp Top Lab Anim Sci* **38**:13–18.
28. Hirst S. 1919. *Studies on acari; no.1, the genus Demodex*, Owen London (United Kingdom): The British Museum. <http://dx.doi.org/10.5962/bhl.title.23700>
29. Hsu CK, Hsu MM, Lee JY. 2009. Demodicosis: a clinicopathological study. *J Am Acad Dermatol* **60**:453–462.
30. Hurley RJ, Desch CE. 1994. *Demodex cricetuli*: new species of hair follicle mite (Acari: Demodicidae) from the Armenian hamster, *Cricetulus migratorius* (Rodentia: Cricetidae). *J Med Entomol* **31**:529–533.
31. Izdebska JN. 2012. A new demodicidae species (Acari) from the yellow-necked mouse *Apodemus flavicollis* (Rodentia: Muridae)—description with data on parasitism. *J Parasitol* **98**:1101–1104.
32. Izdebska JN, Fryderyk S. 2012. New data on the occurrence of *Demodex lacrimalis* (Acari, Demodicidae) of the wood mouse *Apodemus sylvaticus* (Rodentia, Muridae). *Annales Universitatis Mariae Curie-Skłodowska. Sectio C: Biologia* **67**:7–11.
33. Izdebska JN, Kozina P, Gólcz A. 2013. The occurrence of *Demodex* spp. (Acari, Demodicidae) in the bank vole *Myodes glareolus* (Rodentia, Cricetidae) with data on its topographical preferences. *Ann Parasitol* **59**:129–133.
34. Izdebska JN, Rolbiecki L. 2012. Demodectic mites of the brown rat *Rattus norvegicus* (Berkenhout, 1769) (Rodentia, Muridae) with a new finding of *Demodex ratticola* Bukva, 1995 (Acari, Demodicidae). *Ann Parasitol* **58**:71–74.
35. Izdebska JN, Rolbiecki L. 2013. *Demodex microti* n. sp. (Acari: Demodicidae) in *Microtus arvalis* (Pallas) (Rodentia, Cricetidae) with a checklist of the demodectic mites of cricetids. *Syst Parasitol* **86**:187–196.
36. Izdebska JN, Rolbiecki L. 2013. A new species of *Demodex* (Acari: Demodicidae) with data on topical specificity and topography of demodectic mites in the striped field mouse *Apodemus agrarius* (Rodentia: Muridae). *J Med Entomol* **50**:1202–1207.
37. Izdebska JN, Rolbiecki L. 2014. New species of *Demodex* (Acari: Demodicidae) with data on parasitism and occurrence of other Demodectids of *Rattus norvegicus* (Rodentia: Muridae). *Ann Entomol Soc Am* **107**:740–747.
38. Izdebska JN, Rolbiecki L. 2015. A new species of the genus *Demodex* Owen, 1843 (Acari: Demodicidae) from the ear canals of the house mouse *Mus musculus* L. (Rodentia: Muridae). *Syst Parasitol* **91**:167–173.
39. Izdebska JN, Rolbiecki L. 2015. Two new species of *Demodex* (Acari: Demodicidae) with a redescription of *Demodex musculi* and data on parasitism in *Mus musculus* (Rodentia: Muridae). *J Med Entomol* **52**:604–613.
40. Izdebska JN, Rolbiecki L. 2016. A new genus and species of demodectic mites from the tongue of a house mouse *Mus musculus*: description of adult and immature stages with data on parasitism. *Med Vet Entomol* **30**:135–143.
41. Izdebska JN, Rolbiecki L, Fryderyk S. 2016. A new species of *Demodex* (Acari: Demodicidae) from the skin of the vibrissal area of the house mouse *Mus musculus* (Rodentia: Muridae), with data on parasitism. *Syst Appl Acarol* **21**:1031–1039.
42. Institute for Laboratory Animal Research. 2011. *The guide for the care and use of laboratory animals*, 8th ed. Washington (DC): National Academies Press.
43. Jekl V, Hauptman K, Jeklova E, Knotek Z. 2006. Demodicosis in 9 prairie dogs (*Cynomys ludovicianus*). *Vet Dermatol* **17**:280–283.
44. Karlsson EM, Pearson LM, Kuzma KM, Burkholder TH. 2014. Combined evaluation of commonly used techniques, including PCR, for diagnosis of mouse fur mites. *J Am Assoc Lab Anim Sci* **53**:69–73.
45. Koller B, Muller-Wiefel AS, Rupec R, Korting HC, Ruzicka T. 2011. Chitin modulates innate immune responses of keratinocytes. *PLoS One* **6**:1–7.
46. Kunštýř I, Hartmann D. 1983. *Pasteurella pneumotropica* and the prevalence of the AHP (*Actinobacillus*, *Haemophilus*, *Pasteurella*)-group in laboratory animals. *Lab Anim* **17**:156–160.
47. Leithäuser F, Trobonjaca Z, Moller P, Reimann J. 2001. Clustering of colonic lamina propria CD4(+) T cells to subepithelial dendritic cell aggregates precedes the development of colitis in a murine adoptive transfer model. *Lab Invest* **81**:1339–1349.
48. Letscher RM. 1970. Observations concerning the life cycle and biology of *Myobia musculi* (Schränk) and *Myocoptes musculus* (Koch) [MS Thesis], p 84. College Station (TX): Texas A and M University.
49. Liu J, Sheha H, Tseng SC. 2010. Pathogenic role of *Demodex* mites in blepharitis. *Curr Opin Allergy Clin Immunol* **10**:505–510.
50. Liu Q, Arseculeratne C, Liu Z, Whitmire J, Grusby MJ, Finkelman FD, Darling TN, Cheever AW, Swearingen J, Urban JF, Gause

- WC. 2004. Simultaneous deficiency in CD28 and STAT6 results in chronic ectoparasite-induced inflammatory skin disease. *Infect Immun* 72:3706–3715.
51. **Lukoschus FS, Jongman RH.** 1974. *Demodex lacrimalis* spec. nov. (Demodicidae: Trombidiformes) from the Meibomian glands of the European wood mouse *Apodemus sylvaticus*. *Acarologia* 16:274–281.
52. **Luna LG, Armed Forces Institute of Pathology (US).** 1968. Manual of histologic staining methods of the Armed Forces Institute of Pathology, 3rd ed. New York (NY): McGraw–Hill.
53. **Malandro N, Budhu S, Kuhn NF, Liu C, Murphy JT, Cortez C, Zhong H, Yang X, Rizzuto G, Altan-Bonnet G, Merghoub T, Wolchok JD.** 2016. Clonal abundance of tumor-specific CD4<sup>+</sup> T cells potentiates efficacy and alters susceptibility to exhaustion. *Immunity* 44:179–193.
54. **Miller WH, Griffen CE, Campbell KL.** 2012. Muller and Kirk's small animal dermatology, 7th ed. Philadelphia (PA): WB Saunders.
55. **Mitchell R.** 1970. The evolution of a blind gut in trombiculid mites. *J Nat Hist* 4:221–229.
56. **Moats CR, Baxter VK, Pate NM, Watson J.** 2016. Ectoparasite burden, clinical disease, and immune responses throughout fur mite (*Myocoptes musculinus*) infestation in C57BL/6 and *Rag1*<sup>-/-</sup> mice. *Comp Med* 66:197–207.
57. **Mombaerts P, Iacomini J, Johnson RS, Herrup K, Tonegawa S, Papaioannou VE.** 1992. RAG1-deficient mice have no mature B and T lymphocytes. *Cell* 68:869–877.
58. **Moore GJ, Aldred P.** 1978. Treatment of *Pasteurella pneumotropica* abscesses in nude mice (*nu/nu*). *Lab Anim* 12:227–228.
59. **Moriello KA, Newbury S, Steinberg H.** 2013. Five observations of a 3rd morphologically distinct feline *Demodex* mite. *Vet Dermatol* 24:460–462.
60. **Morita E, Kaneko S, Hiragun T, Shindo H, Tanaka T, Furukawa T, Nobukiyo A, Yamamoto S.** 1999. Fur mites induce dermatitis associated with IgE hyperproduction in an inbred strain of mice, NC/Kuj. *J Dermatol Sci* 19:37–43.
61. **Mueller RS, Besignor E, Ferrer L, Holm B, Lemarie S, Paradis M, Shipstone MA.** 2012. Treatment of demodicosis in dogs: 2011 clinical practice guidelines. *Vet Dermatol* 23:86–96. Available at PubMed.
62. **Muranski P, Boni A, Antony PA, Cassard L, Irvine KR, Kaiser A, Paulos CM, Palmer DC, Touloukian CE, Ptak K, Gattinoni L, Wrzesinski C, Hinrichs CS, Kerstann KW, Feigenbaum L, Chan CC, Restifo NP.** 2008. Tumor-specific Th17-polarized cells eradicate large established melanoma. *Blood* 112:362–373.
63. **Nutting WB.** 1976. Hair follicle mites (*Demodex* spp.) of medical and veterinary concern. *Cornell Vet* 66:214–231.
64. **Nutting WB, Satterfield LC, Cosgrove GE.** 1973. *Demodex* spp. infesting tongue, esophagus, and oral cavity of *Onychomys leucogaster*, the grasshopper mouse. *J Parasitol* 59:893–896.
65. **Owen D, Young C.** 1973. The occurrence of *Demodex aurati* and *Demodex criceti* in the Syrian hamster (*Mesocricetus auratus*) in the United Kingdom. *Vet Rec* 92:282–284.
66. **Palopoli MF, Fergus DJ, Minot S, Pei DT, Simison WB, Fernandez-Silva I, Thoemmes MS, Dunn RR, Trautwein M.** 2015. Global divergence of the human follicle mite *Demodex folliculorum*: persistent associations between host ancestry and mite lineages. *Proc Natl Acad Sci USA* 112:15958–15963.
67. **Percy DH, Barthold SW.** 2007. Pathology of laboratory rodents and rabbits, 3rd ed. Ames (IA): Blackwell Publishing.
68. **Pleasant JR.** 1959. Rearing germfree cesarean-born rats, mice, and rabbits through weaning. *Ann N Y Acad Sci* 78:116–126.
69. **Quezada SA, Simpson TR, Peggs KS, Merghoub T, Vider J, Fan X, Blasberg R, Yagita H, Muranski P, Antony PA, Restifo NP, Allison JP.** 2010. Tumor-reactive CD4<sup>+</sup> T cells develop cytotoxic activity and eradicate large established melanoma after transfer into lymphopenic hosts. *J Exp Med* 207:637–650.
70. **Radaelli E, Manarolla G, Pisoni G, Balloi A, Aresu L, Sparaciari P, Maggi A, Caniatti M, Scanziani E.** 2010. Suppurative adenitis of preputial glands associated with *Corynebacterium mastitidis* infection in mice. *J Am Assoc Lab Anim Sci* 49:69–74.
71. **Ricart Arbona RJ, Lipman NS, Wolf FR.** 2010. Treatment and eradication of murine fur mites. II. Diagnostic considerations. *J Am Assoc Lab Anim Sci* 49:583–587.
72. **Ricart Arbona RJ, Lipman NS, Wolf FR.** 2010. Treatment and eradication of murine fur mites. III. Treatment of a large mouse colony with ivermectin-compounded feed. *J Am Assoc Lab Anim Sci* 49:633–637.
73. **Ricart Arbona RJ, Nashat MA, Wolf FR, Lipman NS.** 2016. Estimated prevalence of *Demodex* spp. in a 1600-cage mouse colony and in imported mice from other academic institutions. Abstracts presented at the American Association for Laboratory Animal Science annual meeting, Charlotte, North Carolina, October 30–3 November 2016. *J Am Assoc Lab Anim Sci* 55:693.
74. **Rice KA, Albacarys LK, Metcalf Pate KA, Perkins C, Henderson KS, Watson J.** 2013. Evaluation of diagnostic methods for *Myocoptes musculinus* according to age and treatment status of mice (*Mus musculus*). *J Am Assoc Lab Anim Sci* 52:773–781.
75. **Ríos-Yuil JM, Mercadillo-Perez P.** 2013. Evaluation of *Demodex folliculorum* as a risk factor for the diagnosis of rosacea in skin biopsies. Mexico's General Hospital (1975–2010). *Indian J Dermatol* 58:157.
76. **Ruffi T, Buchner SA.** 1984. T-cell subsets in acne rosacea lesions and the possible role of *Demodex folliculorum*. *Dermatologica* 169:1–5.
77. **Saari SA, Juuti KH, Palojärvi JH, Väisänen KM, Rajaniemi RL, Sajjonmaa-Koulumies LE.** 2009. *Demodex gatoi*-associated contagious pruritic dermatosis in cats—a report from 6 households in Finland. *Acta Vet Scand* 51:40.
78. **Sarre C, Gonzalez-Hernandez A, Van Coppennolle S, Grit R, Grauwet K, Van Meulder F, Chiers K, Van den Broeck W, Geldhof P, Claerebout E.** 2015. Comparative immune responses against *Psoroptes ovis* in 2 cattle breeds with different susceptibility to mange. *Vet Res (Faisalabad)* 46:131.
79. **Sastre N, Francino O, Curti JN, Armenta TC, Fraser DL, Kelly RM, Hunt E, Silbermayr K, Zewe C, Sanchez A, Ferrer L.** 2016. Detection, prevalence and phylogenetic relationships of *Demodex* spp and further skin prostigmata mites (*Acari, Arachnida*) in wild and domestic mammals. *PLoS One* 11:1–20.
80. **Scanziani E, Gobbi A, Crippa L, Giusti AM, Giavazzi R, Cavalletti E, Luini M.** 1997. Outbreaks of hyperkeratotic dermatitis of athymic nude mice in northern Italy. *Lab Anim* 31:206–211.
81. **Scanziani E, Gobbi A, Crippa L, Giusti AM, Pesenti E, Cavalletti E, Luini M.** 1998. Hyperkeratosis-associated coryneform infection in severe combined immunodeficient mice. *Lab Anim* 32:330–336.
82. **Scott DW.** 2012. Letter to the editor: Untreated generalized demodicosis in young dogs. *Vet Dermatol* 23:174–176.
83. **Seyhan ME, Karıncaoğlu Y, Bayram N, Aycan O, Kuku I.** 2004. Density of *Demodex folliculorum* in haematological malignancies. *J Int Med Res* 32:411–415.
84. **Sivajothi S, Sudhakara Reddy B, Rayulu VC.** 2013. Demodicosis caused by *Demodex canis* and *Demodex cornei* in dogs. *J Parasit Dis* 39:673–676.
85. **Smith PC, Zeiss CJ, Beck AP, Scholz JA.** 2016. *Demodex musculi* infestation in genetically immunomodulated mice. *Comp Med* 66:278–285.
86. **Tani K, Iwanaga T, Sonoda K, Hayashiya S, Hayashiya M, Taura Y.** 2001. Ivermectin treatment of demodicosis in 56 hamsters. *J Vet Med Sci* 63:1245–1247.
87. **Tani K, Une S, Hasegawa A, Adachi M, Kanda N, Watanabe S, Nakaichi M, Taura Y.** 2005. Infestivity of *Demodex canis* to hamster skin engrafted onto SCID mice. *J Vet Med Sci* 67:445–448.
88. **Ullman-Culleré MH, Foltz CJ.** 1999. Body condition scoring: a rapid and accurate method for assessing health status in mice. *Lab Anim Sci* 49:319–323.
89. **van den Broek AH, Else RW, Huntley JF, Machell J, Taylor MA, Miller HR.** 2004. Early innate and longer-term adaptive cutaneous immunoinflammatory responses during primary infestation with the sheep scab mite, *Psoroptes ovis*. *J Comp Pathol* 131:318–329.
90. **Walton SF.** 2010. The immunology of susceptibility and resistance to scabies. *Parasite Immunol* 32:532–540.

91. **Zhao YE, Hu L, Wu LP, Ma JX.** 2012. A meta-analysis of association between acne vulgaris and *Demodex* infestation. *J Zhejiang Univ Sci B* **13**:192–202.
92. **Zhao YE, Wu LP, Hu L, Xu JR.** 2012. Association of blepharitis with *Demodex*: a meta-analysis. *Ophthalmic Epidemiol* **19**:95–102.
93. **Zhao YE, Xu JR, Hu L, Wu LP, Wang ZH.** 2012. Complete sequence analysis of 18S rDNA based on genomic DNA extraction from individual *Demodex* mites (Acari: Demodicidae). *Exp Parasitol* **131**:45–51.